

## ***In vivo* serial joint space measurements during dynamic loading in a canine model of osteoarthritis<sup>1</sup>**

W. J. Anderst M.S.\*, C. Les D.V.M., Ph.D. and S. Tashman Ph.D.

Motion Analysis Lab, Bone and Joint Center, Henry Ford Hospital, Detroit, MI 48202, USA

### **Summary**

**Objective:** To devise a reliable, sensitive method to measure joint space *in vivo* during dynamic loading. Additionally, to determine if dynamic joint space changes were related to the severity of long-term cartilage damage.

**Design:** Subjects were 23 adult foxhounds (18 experimental, 5 control). Experimental subjects had surgically transected cranial cruciate ligaments (CCL). Dynamic joint space was serially measured *in vivo* over 2 years using a unique high speed stereo radiographic system in combination with subject-specific computed tomography reconstructions.

**Results:** Dynamic joint space was measured *in vivo* with a within-day precision of 0.09 mm. Half of the experimental subjects developed minor articular cartilage damage and the other half developed severe articular cartilage damage in the medial knee compartment. Joint space during treadmill running increased significantly in the minor damage group in both the medial (+0.61 mm,  $P = 0.036$ ) and lateral (+0.84 mm,  $P = 0.002$ ) compartments of the knee. Dynamic joint space in the severe damage group did not increase significantly on either the medial (+0.27 mm,  $P = 0.408$ ) or lateral (+0.44 mm,  $P = 0.199$ ) side. The majority of the change in joint space occurred the first year after CCL transection. Medial meniscus damage was related to severity of medial articular cartilage damage ( $\tau = 0.447$ ,  $P = 0.003$ ). The minor damage group developed 73% of all osteophytes noted at dissection.

**Conclusions:** This technique is a precise tool for measuring joint space serially *in vivo* under dynamic loading conditions. The data suggest decreased severity in long-term articular cartilage damage is related to: osteophyte formation, less severe medial meniscus damage and increased joint space the first 12 months after injury.

© 2005 OsteoArthritis Research Society International. Published by Elsevier Ltd. All rights reserved.

**Key words:** Cartilage thickening, Functional joint space, Anterior cruciate ligament.

### **Introduction**

Joint space narrowing is commonly used to infer articular cartilage loss, and is the recommended outcome measure for anatomical progression of disease<sup>1,2</sup>. However, reliable, sensitive measurements of cartilage loss during the progression of osteoarthritis (OA) have been difficult to obtain. In the past, serial measurements of joint space narrowing were unreliable due to the difficulty in precisely repositioning patients and radiographic equipment<sup>3,4</sup>. This unreliability led to differences in joint space measurements that were not necessarily the result of cartilage changes, but instead were likely related to knee flexion and the inherent differential thickness in articular cartilage in the femoral and tibial condyles<sup>5</sup>. However, a more recently developed protocol for standardized knee radiographs yields increased reliability in static joint space measurements<sup>6,7</sup>.

Magnetic resonance imaging (MRI) has increasingly been used as an alternative to static radiographs for identifying and quantifying OA<sup>8,9</sup>. MRI measurements of articular cartilage volume have been shown to be highly repeatable<sup>10,11</sup>. However, it has been suggested that serial

measurements of total cartilage volume may be unable to track the structural changes that occur with OA<sup>12</sup>.

Conventional radiographic and MRI measurements still have shortcomings when measuring joint space. Most notably, joint space data are not collected as the joint is dynamically loaded. Thus, conventional radiographic and MRI protocols measure joint space along only one line of contact and do not account for differences in articular cartilage thickness over the entire contact region during active motion. Additionally, the response of articular cartilage and the meniscus to dynamic loads such as those encountered during walking and running cannot be quantified from static radiographs and MRI.

The present study serially measured joint space in canines. Dogs have long been used to study joint degeneration and the development of OA<sup>13</sup>. Transection of the cranial cruciate ligament (CCL), analogous to the anterior cruciate ligament in humans, leads to joint degeneration, cartilage loss and the development of OA<sup>14–17</sup>. It is believed that CCL transection leads to instability and eventually promotes mechanically induced OA<sup>18</sup>, resulting in morphological and biochemical changes that are indistinguishable from those of the natural disease<sup>19</sup>. The rate at which OA develops in dogs appears to be highly variable, as it is in humans<sup>20,21</sup>, and the reaction to the instability differs markedly among different anatomical areas of the joint<sup>22</sup>. Previous research has documented ground reaction force changes<sup>23</sup> as well as kinematic changes in canine gait after CCL transection<sup>24–26</sup>. However, none of these

<sup>1</sup> Sources of support: National Institutes of Health grant AR43860.

\*Address correspondence and reprint requests to: William J. Anderst, Motion Analysis Lab, Henry Ford Hospital, ER2015, Detroit, MI 48202, USA. Tel: 1-313-916-8684; E-mail: [anderst@bjc.hfh.edu](mailto:anderst@bjc.hfh.edu)

Received 10 October 2004; revision accepted 22 April 2005.

measures were shown to be related to the rate or magnitude of cartilage damage.

The purpose of this research was twofold: first, to devise a reliable, sensitive method to measure joint space *in vivo* while the joint was dynamically loaded; and second, to determine if serial changes in joint space measurements were related to the severity of long-term cartilage damage in the CCL deficient dog model.

**Methods**

Our Institutional Animal Care and Use Committee approved all animal testing and procedures prior to commencing the study. Twenty-three skeletally mature (2–3 years old) female foxhounds served as subjects. A minimum of three 1.6 mm diameter tantalum beads were implanted into both the right distal femur and proximal tibia at the beginning of the study. Testing commenced 4 weeks after bead implant surgery and consisted of running on a treadmill set at 1.5 m/s. During the treadmill running, the dogs were X-rayed using a unique stereo radiographic imaging system capable of tracking the implanted beads with an accuracy of better than  $\pm 0.10$  mm (Tashman and Anderst<sup>27</sup>). All dogs underwent a second surgery after the first test session. Eighteen dogs received a complete transection of the CCL, while five dogs underwent a sham operation in which the CCL was exposed but not transected. Dogs returned to full activity within 2 months after

the second surgery and received regular exercise throughout the study (30 min of treadmill running three times per week). The dogs were tested running on the treadmill nine more times (2, 4, 6, 8, 10, 12, 16, 20 and 24 months after the second surgery). Three trials of treadmill running were collected during each test session, and the average of the three trials was used as the measurement for the test session.

Two synchronized video cameras collected X-ray images at 250 frames/s starting 0.2 s prior to pawstrike and ending 0.4 s after pawstrike. The two-dimensional locations of the implanted beads were determined for each camera frame using custom designed software. The two-dimensional bead locations were input to commercial software (Eva, Motion Analysis Corp.) for tracking and three-dimensional (3D) reconstruction. The resulting 3D bead coordinates were smoothed using a fourth-order zero-lag Butterworth low pass filter with a cutoff frequency of 25 Hz. Data from pawstrike to 0.20 s after pawstrike were included in the final data analysis.

Dynamic joint space was determined by finding the minimum distance between subchondral bone surfaces for each frame of data. To determine these joint space values, computed tomography (CT) data were collected at the completion of the study (1 mm slices, 0.488 mm  $\times$  0.488 mm resolution). The CT slices were reconstructed into 3D wireframe meshes consisting of triangular elements<sup>28</sup> [Fig. 1(a)]. Each bone surface triangle's centroid and area ( $<1$  mm<sup>2</sup>, on average) were calculated. The CT

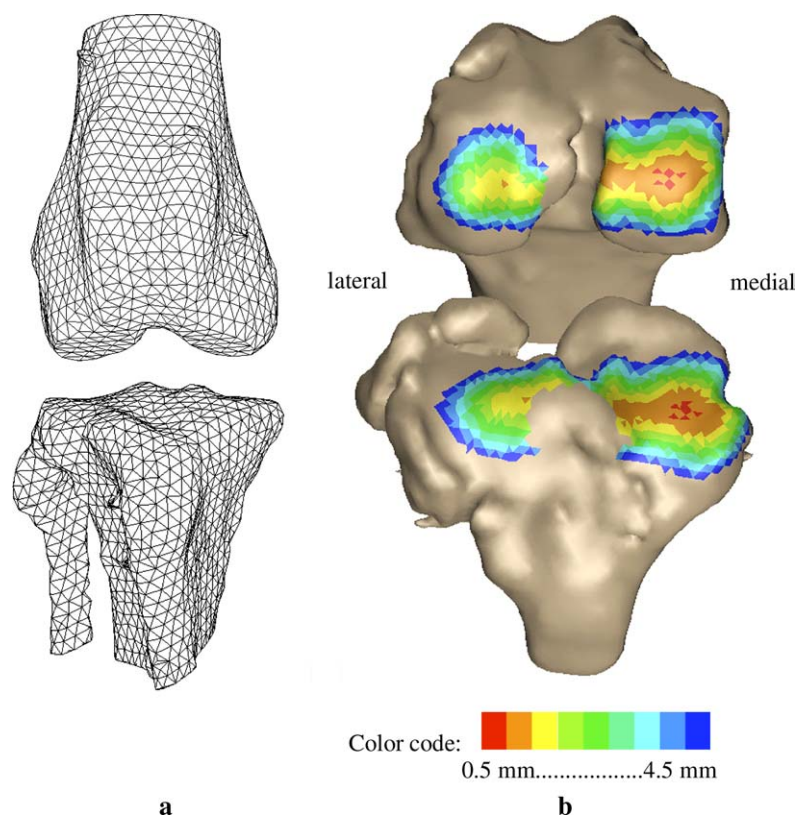


Fig. 1. Reconstructed bones and distance maps. (a) The surface mesh for the femur (top) and tibia (bottom). (b) The articulating surfaces of the femur (top) and tibia (bottom), with the joint “opened up”. Surface triangles were colored according to their minimum distance to the opposing bone surface. Color variations represent 0.5 mm changes in distance between subchondral bone surfaces, starting with surfaces  $\leq 0.5$  mm apart colored red and ending with surfaces  $\leq 4.5$  mm apart colored dark blue.

scans provided the locations of the beads within each 3D reconstructed bone. Combining the 3D bead coordinates within the CT reconstructions with the 3D bead coordinates obtained from the radiographic image pairs, the bone reconstructions were located and oriented precisely as they were during the treadmill running. The minimum distance between opposing subchondral bone surface triangle centroids was then calculated for each frame of data [Fig. 1(b)]. The intercondylar eminence on the tibia and the region between the femoral condyles were not included in the minimum distance calculations. Although these regions were occasionally close to the opposing articulating bone surface, it was assumed that significant load bearing contact did not occur in these regions. More details on this method have been previously published<sup>29</sup>.

The distance between subchondral bone surfaces continually changed as the applied load and joint orientation changed. A single parameter, called the functional joint space (FJS) score, was created to quantify this continuously changing relationship. Determining FJS scores was a three-step process. First, the minimum distance between subchondral bone surfaces was determined at each triangular element for each frame of data [Fig. 2(a)]. Second, the overall minimum distance to the opposing bone surface was determined for each triangular element, taking into account all frames of data (the minimum of all the

instantaneous minimums). This resulted in an overall minimum distance map [Fig. 2(b)]. Third, the overall minimum distance map was used to calculate the FJS score. FJS scores were calculated for each compartment (medial and lateral) on each bone (femur and tibia) for all dogs on all test days [Fig. 2(c)]. The FJS score was calculated by creating an ordered list of the triangular surface elements from the overall minimum distance map. The ordered list started with the elements closest to the opposing surface [red in Fig. 2(b)] and ended with the elements farthest from the opposing surface [blue in Fig. 2(b)]. Each triangular element had an associated surface area and distance value. While proceeding down the ordered list of triangular elements, the area of each element was added to the total surface area. This process was continued until the total surface area reached 200 mm<sup>2</sup>. At that point, the average distance value of the triangular elements making up the closest 200 mm<sup>2</sup> area was determined (the distance value of each triangular element was weighted by the surface area of each element). This average distance value of the closest 200 mm<sup>2</sup> area was the FJS score. A smaller FJS score indicated less joint space.

A surface area of 200 mm<sup>2</sup> was selected because the variability in FJS score using this region was low, it was big enough to include relatively large regions of cartilage loss, it

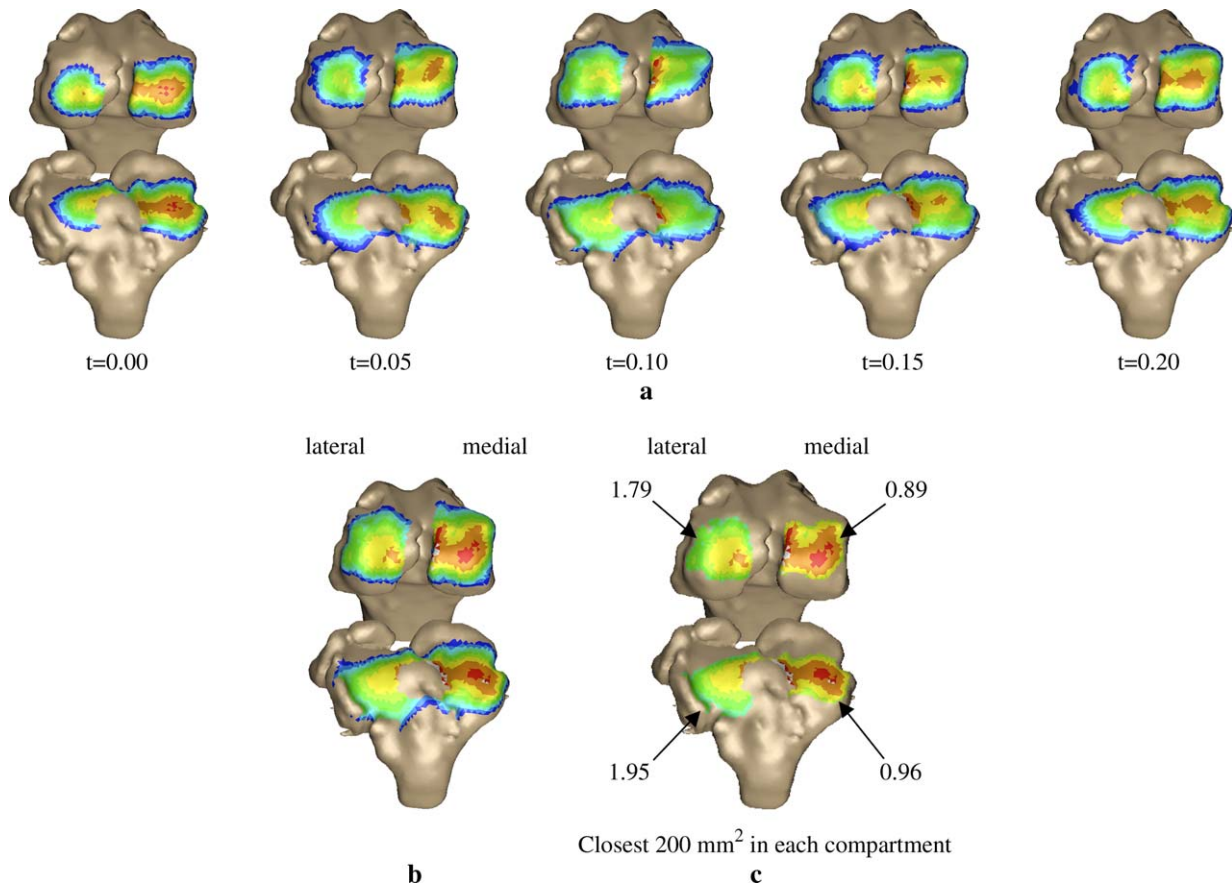


Fig. 2. Calculating FJS score. (a) Minimum distance maps for five instants of the analyzed motion. Time  $t = 0.00$  s was the time of pawstrike. (b) The overall minimum distance map, showing the closest values for every surface triangle during the entire motion (pawstrike to 0.20 s after pawstrike). (c) FJS scores using the closest 200 mm<sup>2</sup> area within each compartment (medial and lateral femur; medial and lateral tibia). Color scale is the same as Fig. 1(b), plus white triangles indicate overlap of subchondral joint surfaces.



was large enough to account for cartilage thickness differences in various areas of the joint<sup>22</sup>, and it was less likely than smaller areas to have the score affected by small irregularities in the calculated close-contact region (such as along the slope of the intercondylar eminence on the tibia, an unlikely weightbearing region).

Precision was measured by calculating the within-day standard deviation of all FJS scores. This included measurements from all 10 test days of all 23 dogs. Typically, three trials were included per dog per day. The effect of time on medial and lateral FJS scores relative to pre-transection data was assessed with repeated measures ANOVAs. Best-fit lines were calculated for both the medial FJS and lateral FJS data for each subject for the second to twelfth month post-injury, and the slopes of these lines were tested by ANOVA for differences among groups. Least significant difference tests were performed for all *post hoc* tests. All statistical tests were two-tailed with significance set at  $P < 0.05$ .

A small bias within each CT scan reconstruction required statistical comparisons to be made within-dog and relative to pre-transection data. CT scan slice spacing of 1 mm resulted in a bias in the reconstruction of the bone of up to 1 mm, depending on how close the final slice was to the actual end of the subchondral bone. This bias likely varied

with each bone CT scan. However, the same subject-specific CT reconstruction was used on each test date. In this way, all data could be compared to the pre-transection data within each dog and changes could be accurately measured. Due to the possible bias in CT reconstructions, it was inappropriate to compare actual FJS values between subjects, as the amount of subchondral bone skipped between the last CT scan slice and the actual end of the bone was unknown.

At sacrifice, tibia and femur articulating surfaces were stained with India ink to identify location, size and severity of cartilage damage. Photos of all articulating surfaces (stained and unstained) were viewed by one of the authors (CML) and graded on a five-point scale according to cartilage damage, similar to that which has been used previously<sup>30</sup> (0 = no damage; 1 = visible surface damage/fibrillation; 2 = small regions of thinned cartilage, no full thickness defects; 3 = large regions of thinned cartilage and/or small full thickness defects; 4 = large regions of full thickness cartilage loss). Grades were recorded for each compartment (medial and lateral) on each bone (Fig. 3, top). Overall, cartilage damage variability was small on the lateral side. Thus, dogs were grouped for statistical tests according to the extent of medial compartment damage, determined by adding the medial tibia and femur cartilage damage grades.

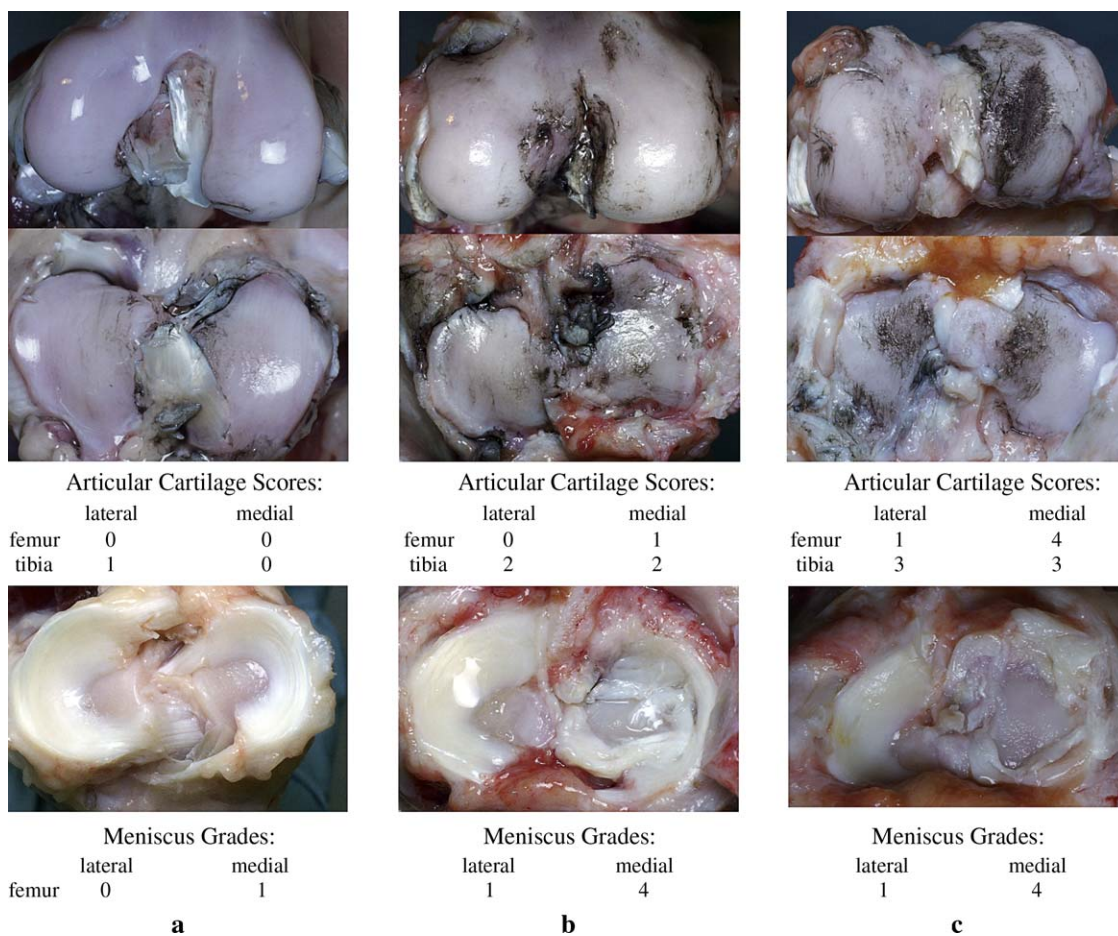


Fig. 3. India ink staining of articulating surfaces (top) and meniscal photos (bottom). (a) A joint with little or no cartilage damage and an intact meniscus. (b) A joint with minor cartilage damage and torn medial meniscus. (c) A joint with severe cartilage damage and destroyed medial meniscus. Scores for each compartment are displayed under the respective photographs.

Dogs with medial compartment grades (femur + tibia) less than 2 were in the no damage group ( $n = 5$ ; all control dogs), medial compartment grades from 2 to 4 ( $n = 9$ ) were in the minor damage group and medial compartment grades from 5 to 8 ( $n = 9$ ) made up the major damage group.

Meniscal status was noted at time of dissection and photos of tibia articular surfaces were taken prior to removing the meniscus. A meniscal status grade was determined for each compartment using dissection notes and photos (Fig. 3, bottom). The criteria for menisci grades were identical to a scale used previously<sup>31</sup> (0 = normal; 1 = longitudinal surface striations; 2 = longitudinal surface tears; 3 = penetrating longitudinal tears producing a loose piece of tissue attached at both ends (a bucket handle tear); 4 = transverse tears producing a loose tissue flap, fibrillation of the entire meniscus, or absence of the meniscus). Kendall's tau correlations were used to calculate the relationship between articular cartilage damage (femur + tibia articular damage score) and meniscal status score for both the medial and lateral compartments.

Osteophyte formation was noted at time of dissection. Osteophyte location (medial/lateral) and associated bone (femur/tibia) were recorded.

## Results

Femur and tibia FJS scores were highly correlated within each compartment (medial  $r = 0.94$ ; lateral  $r = 0.88$ ). Due to the high correlations, average values were used for the medial compartment (the average of the medial femur and medial tibia score) and the lateral compartment (the average of the lateral femur and lateral tibia score) in all statistical tests.

The within-day variability in FJS score for all 23 dogs covering 10 test sessions for each dog was 0.09 mm for both the lateral and medial compartments.

Prior to surgery, medial compartment FJS scores overall averaged  $0.60 \pm 0.73$  mm (mean  $\pm$  SD) while lateral compartment FJS scores averaged  $1.45 \pm 0.85$  mm. Medial FJS scores in the control group decreased slightly

( $-0.24$  mm,  $P = 0.490$ ) over the 2-year test period (Fig. 4). Dogs with minor articular cartilage damage showed increased FJS scores in the medial compartment (0.61 mm,  $P = 0.036$ ), with FJS scores on the 20- and 24-month post-transection test dates significantly different from scores at the 2- and 4-month post-transection tests (Fig. 4). Dogs that displayed severe cartilage damage at the end of the study developed a small (0.27 mm,  $P = 0.408$ ), non-significant increase in FJS in the medial compartment relative to pre-surgery (Fig. 4).

Lateral FJS scores increased slightly (0.18 mm,  $P = 0.440$ ) in the control group (Fig. 5). Subjects with minor cartilage damage exhibited a decrease in FJS in the lateral compartment 2 months after surgery ( $-0.32$  mm,  $P = 0.219$ ), followed by significant increases in lateral FJS starting 8 months post-transection ( $P = 0.007$ ) and continuing until the end of the study ( $P < 0.001$ ). Dogs with severe cartilage damage showed an initial decrease in FJS in the lateral compartment 2 months after surgery ( $-0.41$  mm,  $P = 0.202$ ) and then a consistent increase in FJS through the 16-month post-transection test date (Fig. 5).

The majority of the change in FJS recorded in the experimental dogs occurred the first year after CCL transection. However, the rate of change in FJS in the medial compartment the first 12 months after surgery was not significantly different between the severe and minor damage groups ( $P = 0.07$ ). Likewise, the rate of change in lateral compartment FJS was not significantly different between severe and minor damage groups ( $P = 0.08$ ) from the second to twelfth month post-surgery.

Severe medial meniscal damage was found in 14 of the 18 experimental dogs in this study. Medial meniscal damage was related to the severity of medial articular surface damage (Table I) (Kendall's tau = 0.447,  $P = 0.003$ ). Only three experimental dogs developed lateral meniscal destruction. There was not a statistically significant relationship between lateral meniscal damage and the severity of lateral compartment articular surface damage (Table II) (Kendall's tau = 0.225,  $P = 0.132$ ).

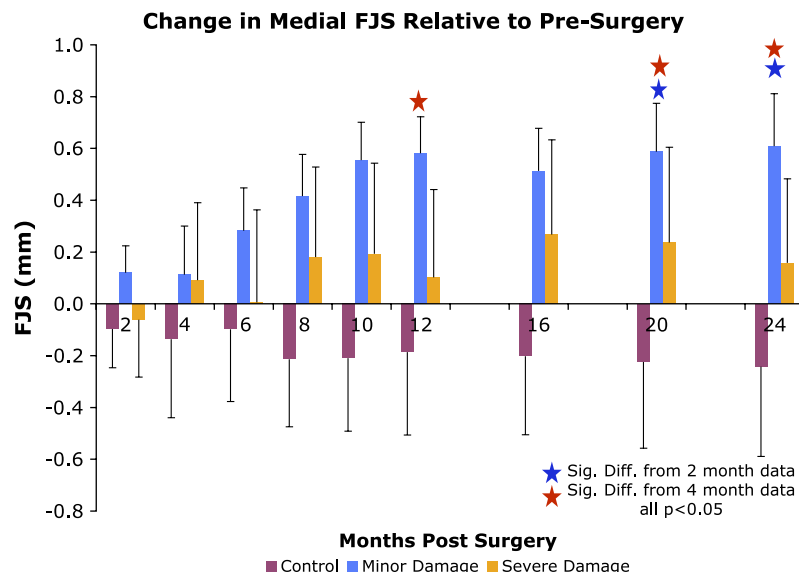


Fig. 4. Change in medial FJS scores ( $\pm$  standard error) relative to pre-CCL transection.

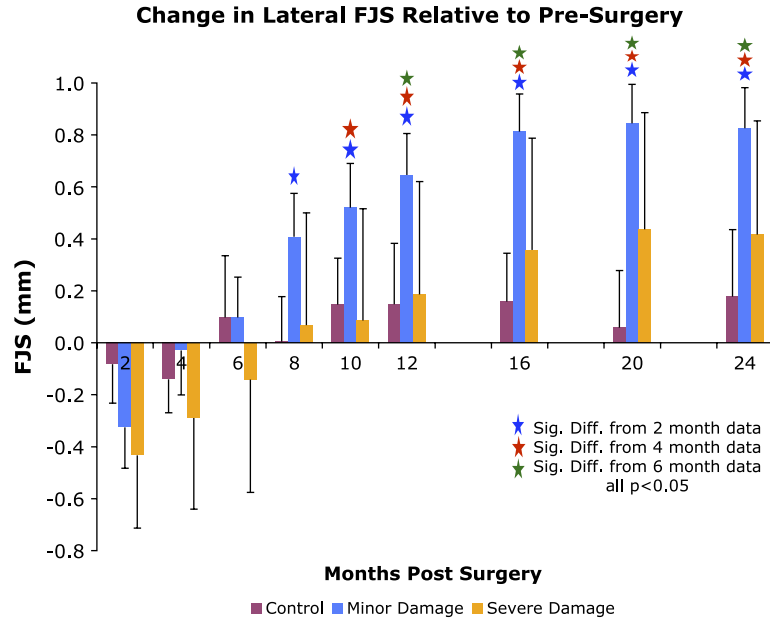


Fig. 5. Change in lateral FJS scores ( $\pm$  standard error) relative to pre-CCL transection.

No osteophytes were noted in any of the control dogs or on any of the contralateral limbs for any dogs. Nineteen of the 26 osteophyte notations pertained to dogs in the minor damage group. Fifteen osteophytes were noted as being associated with the femur, 11 with the tibia.

**Discussion**

A significant limitation to static joint space measurements is that it is not possible to measure meniscal and articular cartilage response to dynamic loads. Additionally, during a static measurement, minimum joint space is calculated only for the regions in contact at one particular joint orientation. Similarly, measuring joint space at a specific instant (or joint angle) during a dynamic motion quantifies

the joint space at one single instant or one configuration. Selection of the most appropriate instant to study may be problematic in the knee in particular, as joint space does not necessarily change simultaneously in the two compartments. The new concept presented here, FJS, quantifies minimum joint space during the impact and loading phase of dynamic joint motion and accounts for different surface regions coming into contact and the response of articular cartilage and meniscus to load. The result is a true 3D minimum distance map of all contacting surfaces.

As noted in the results, the average precision in FJS scores for all 10 test sessions of all 23 dogs was 0.09 mm. This result is comparable to the most precise static joint space measurements in humans where the median standard deviation in minimum medial joint space width for test–retest film pairs was 0.08 mm (Dupuis *et al.*<sup>6</sup>) and 0.09 mm (Buckland-Wright *et al.*<sup>7</sup>).

Table I

Medial compartment meniscal damage and articular cartilage damage scores

		Medial Compartment Articular Cartilage Damage								
		0	1	2	3	4	5	6	7	8
Medial Meniscal Damage	0	●	●	●						
	1	●	●							
	2			□			▲			
	3					□				
	4			□	□	□	□	▲	▲	▲

● = control group, □ = minor articular cartilage damage, ▲ = major articular cartilage damage.

Table II

Lateral compartment meniscal damage and articular cartilage damage scores

		Lateral Compartment Articular Cartilage Damage								
		0	1	2	3	4	5	6	7	8
Lateral Meniscal Damage	0	●	●		▲	▲				
	1	●	●	□	□	□	▲			
	2			□	□	□	▲			
	3									
	4				□	▲	▲			

● = control group, □ = minor articular cartilage damage, ▲ = major articular cartilage damage.

Medial cartilage thickness (femur + tibia) in 40-week-old beagles has been found to range from approximately 1.48 mm to 1.64 mm and lateral cartilage thickness ranged from approximately 0.95 mm to 1.08 mm (Kiviranta *et al.*<sup>32</sup>). Cartilage thickness on the weightbearing surface of adult dogs 36 months post-transection has been measured to be between 0.3 mm and 1.2 mm on the medial femoral condyle, and between 0.5 mm and 1.8 mm on the lateral femoral condyle<sup>33</sup>. The present data are more closely in agreement with the latter findings: our technique found the medial FJS to be consistently smaller than the lateral FJS, and thus it can be inferred that the medial compartment cartilage and meniscus was thinner and/or more compressed than the lateral compartment cartilage and meniscus during dynamic loading.

The data in Figs. 4 and 5 indicate the medial FJS slightly decreased while the lateral FJS slightly increased for the control dogs over the 2-year test period. These changes over 2 years were not statistically significant and the trends are likely the result of the normal aging process.

Numerous researchers have previously found evidence of cartilage hypertrophy in unstable canine knees<sup>19,22,33–37</sup>. Cartilage hypertrophy may result from increased hydration<sup>38</sup> and swelling<sup>19</sup>, increased synthesis of matrix components<sup>33</sup>, increased biosynthesis, perhaps mediated through an increase in the amount of growth factors or other anabolic factors<sup>22</sup>, and bony remodeling associated with the expansion of femoral condyles<sup>36</sup>. Increased cartilage thickness or volume has been found in CCL transected joints 6 weeks<sup>19</sup>, 8 months<sup>34</sup>, 64 weeks<sup>35,36</sup>, 36 months<sup>37</sup> and 45 months<sup>33</sup> post-transection. Changes in FJS score over time (Figs. 4 and 5) as assessed *in vivo* under dynamic loading are consistent with these previously published results. An increase in FJS was evident in both the medial and lateral compartments after CCL transection. The initial decrease in lateral FJS following ligament transection was likely due to the drastically changed kinematics<sup>27</sup> and the accompanying change in regions of close contact at the articulating surfaces rather than an immediate decrease in articular cartilage or meniscal thickness. The increased FJS scores in the medial (0.61 mm) and lateral compartments (0.84 mm) in the minor damage group were substantial considering the peak cartilage thickness (femur + tibia) in the weightbearing canine knee is likely less than 2.5 mm.

Figures 4 and 5 reveal that for each of the CCL transected groups there were two phases in response to CCL transection. The early phase lasted from transection to 12 or 16 months post-transection. During this phase there was a fairly steady increase in FJS, and the change reached significance in the minor damage group by the eighth month after transection. The second phase began 12 or 16 months after transection and was characterized by relatively constant FJS scores in each compartment. Several researchers have noted that cartilage hypertrophy appeared to be an initial event preceding cartilage breakdown<sup>33,34</sup>. The present results suggest 12 to 16 months post-transection is the point at which joint space decreasing factors (such as cartilage breakdown) begin to match the rate of joint space increasing factors (such as hypertrophy).

One year after CCL transection the minor damage group had significantly increased FJS relative to the first post-transection measurements in both the medial and lateral compartments. The major damage group, on the other hand, did not significantly increase FJS relative to the first post-transection tests during the 2 years of testing. These

results imply that the biologic response to CCL transection during the first year post-transection is associated with the severity of long-term articular cartilage damage.

Factors that may have contributed to slow the increase in FJS after CCL transection include a deteriorated meniscus<sup>31</sup>, increased compliance of the articular cartilage during compression<sup>38</sup>, and articular cartilage breakdown. Differences between medial and lateral meniscal damage may explain both the greater medial compartment articular cartilage damage and the smaller increase in FJS in the medial compartment (compared to the lateral compartment) measured in the experimental dogs. Medial meniscal deterioration led to less medial joint space, and likely increased pressure on the articular cartilage within the medial compartment. The increased pressure on the medial compartment may have reduced the effects of hypertrophy and swelling, and increased the rate of articular cartilage degeneration. The result of this sequence of events was full thickness cartilage loss on the medial side in some subjects. FJS scores cannot pinpoint the time at which the medial meniscus reached the point where it was no longer functionally useful, however previous research has found that medial meniscus damage reached the level of grade 3 or 4 in 83% of dogs after 32 weeks following CCL transection<sup>31</sup>.

The long-term increase in FJS score for the minor damage group suggests that the cartilage hypertrophy that followed CCL transection was an actual increase in functional thickness. The measurements presented here were obtained *in vivo* under dynamic loading. Thus, the present results demonstrate that even if the hypertrophied cartilage was more compliant, the functional thickness still increased in dogs that developed only minor articular cartilage damage.

There are limitations to the FJS score calculations presented here. First, the FJS method cannot precisely determine the magnitude of each joint space altering factor, such as hypertrophy, swelling, meniscal deterioration or articular cartilage loss. Only an overall change in FJS can be determined using the FJS method. Second, CT scans were acquired at the end of the present study. Thus, osteophytes were included in all CT reconstructions, even if the bone alterations did not develop until the latter portion of the study. Inclusion of osteophytes on test dates when they had not yet formed resulted in lower FJS scores only if the osteophytes were in the region of closest contact. The effect of this limitation can be reduced in future studies if CT scans are collected both at the beginning and end of the study.

Further investigation on dynamic joint space data may produce additional insights into the development of OA. A future objective is to identify specific regional changes in functional space within each compartment. As previous research has noted, the hypertrophic response varies significantly among different areas of the joint<sup>22,33</sup>, with cartilage increasing less in the constantly loaded surface regions. Regional FJS changes may be obtained by calculating the differences between the first and last test overall distance maps or by dividing each articular surface into subregions and identifying changes in dynamic joint space within each subregion. Additionally, a mechanical description of the interaction between joint surfaces, including the magnitude and direction of sliding and rolling contact within each compartment, may provide an explanation as to why articular cartilage and the meniscus change in specific anatomic locations.

In conclusion, the FJS method to quantify dynamic joint space *in vivo* produced repeatable measurements with low



variability, making it a useful tool for serial studies. Additionally, unlike previously published studies, these joint space measurements were acquired *in vivo* as the joint was dynamically loaded and moved through a range of motion. Thus, the changing orientation between the articulating surfaces, the variable forces acting on the joint during loading, and the deformation of the cartilage and meniscus were all taken into account. The results suggest decreased severity in long-term articular cartilage damage is associated with increased osteophyte formation and less severe medial meniscus damage. Additionally, dogs with minor long-term damage increased FJS within 12 months after ligament transection, while dogs with severe long-term damage did not increase FJS. Thus, adaptations that protect the cartilage (or conversely damage that eventually destroys the cartilage) occur relatively quickly after CCL transection.

## References

- Altman RD, Fries JF, Bloch DA, Carstens J, Cooke TD, Genant H, *et al.* Radiographic assessment of progression in osteoarthritis. *Arthritis Rheum* 1987; 30(11):1214–25.
- Lequesne M, Brandt K, Bellamy N, Moskowitz R, Menkes C, Pelletier J-P, *et al.* Guidelines for testing slow acting drugs in osteoarthritis. *J Rheumatol* 1994; 21(Suppl 41):65–73.
- Mazucca SA, Brandt KD, Buckland-Wright C, Buckwalter KA, Katz BP, Lynch JA, *et al.* Field test of the reproducibility of automated measurements of medial tibiofemoral joint space width derived from standardized knee radiographs. *J Rheumatol* 1999; 26(6):1359–65.
- Peterfy C, Li J, Zaim S, Duryea J, Lynch J, Miaux Y, *et al.* Comparison of fixed-flexion positioning with fluoroscopic semi-flexed positioning for quantifying radiographic joint-space width in the knee: test–retest reproducibility. *Skeletal Radiol* 2003;32:128–32.
- Deep K, Norris M, Smart C, Senior C. Radiographic measurement of joint space height in non-osteoarthritic tibiofemoral joints. *J Bone Joint Surg Br* 2003;85-B: 980–2.
- Dupuis DE, Beynon BD, Richard MJ, Novotny JE, Skelly JM, Cooper SM. Precision and accuracy of joint space width measurements of the medial compartment of the knee using standardized MTP semi-flexed radiographs. *Osteoarthritis Cartilage* 2003;11: 716–24.
- Buckland-Wright JC, Ward RJ, Peterfy C, Mojcik CF, Leff RL. Reproducibility of the semiflexed (metatarsophalangeal) radiographic knee position and automated measurements of medial tibiofemoral joint space width in a multicenter clinical trial of knee osteoarthritis. *J Rheumatol* 2004;31(8):1588–97.
- Cicuttini FM, Wluka AE, Forbes A, Wolfe R. Comparison of tibial cartilage volume and radiological grade of the tibiofemoral joint. *Arthritis Rheum* 2003;48(3): 682–8.
- Jones G, Changhai D, Scott F, Glisson A, Cicutti F. Early radiographic osteoarthritis is associated with substantial changes in cartilage volume and tibial bone surface area in both males and females. *Osteoarthritis Cartilage* 2004;12:169–74.
- Eckstein F, Westhoff J, Sitttek H, Maag KP, Haubner M, Faber, *et al.* *In vivo* reproducibility of three-dimensional cartilage volume and thickness measurements with MR imaging. *AJR Am J Roentgenol* 1998;170(3): 593–7.
- Burgkart R, Glaser C, Hyhlik-Durr A, Englmeier KH, Reiser M, Ekstein F. Magnetic resonance imaging-based assessment of cartilage loss in severe osteoarthritis. *Arthritis Rheum* 2001;44(9):2072–7.
- Gandy SJ, Dieppe PA, Keen MC, Maciewicz RA, Watt I, Waterton JC. No loss of cartilage volume over three years in patients with knee osteoarthritis as assessed by magnetic resonance imaging. *Osteoarthritis Cartilage* 2002;10:929–37.
- Pond MJ, Nuki G. Experimentally induced osteoarthritis in the dog. *Ann Rheum Dis* 1973;32:387–8.
- Altman R, Tenenbaum J, Latta L, Riskin W, Blanco LN, Howell DS. Biomechanical and biochemical properties of dog cartilage in experimentally produced osteoarthritis. *Ann Rheum Dis* 1984;43:83–90.
- O'Connor BL, Oates K, Gardner DL, Middleton JFS, Orford CR, Brereton JD. Low temperature and conventional scanning electron microscope observations of dog femoral condylar cartilage surface after anterior cruciate ligament division. *Ann Rheum Dis* 1985;44:321–7.
- Pidd JG, Gardner DL, Adams ME. Ultrastructural changes in femoral condylar cartilage of mature American foxhounds following transection of the anterior cruciate ligament. *J Rheumatol* 1988;15: 663–9.
- Guilak F, Radcliff A, Lane N, Rosenwasser MP, Mow VC. Mechanical and biochemical changes in the superficial zone of articular cartilage in canine experimental osteoarthritis. *J Orthop Res* 1994;12: 474–84.
- Brandt KD, Myers SL, Burr D, Albrecht M. Osteoarthritic changes in canine articular cartilage, subchondral bone, and synovium fifty-four months after transection of the anterior cruciate ligament. *Arthritis Rheum* 1991; 34(12):1560–70.
- McDevitt C, Gilbertson E, Muir H. An experimental model of osteoarthritis; early morphological and biochemical changes. *J Bone Joint Surg* 1977;59B: 24–35.
- Spector TD, Dacre JE, Harris PA, Huskisson EC. Radiological progression of osteoarthritis: an 11-year follow up study of the knee. *Ann Rheum Dis* 1992;51: 1107–10.
- Lequesne M. Quantitative measurement of joint space during progression of osteoarthritis: 'chondrometry'. In: Kuettner K, Goldberg V, Eds. *Osteoarthritic Disorders*. Rosemont: American Academy of Orthopaedic Surgeons 1995;Volume 30:427–44.
- Adams ME. Cartilage hypertrophy following canine anterior cruciate ligament transection differs among different areas of the joint. *J Rheumatol* 1989;16(6): 818–24.
- O'Connor BL, Visco DM, Heck DA, Meyers SL, Brandt KD. Gait alterations in dogs after transection of the anterior cruciate ligament. *Arthritis Rheum* 1989;32(9): 1142–7.
- Korvick DL, Pijanowski GJ, Shaeffer DJ. Three-dimensional kinematics of the intact and cranial cruciate ligament-deficient stifle of dogs. *J Biomech* 1994;27(1):77–87.
- Vilensky JA, O'Connor BL, Brandt KD, Dunn EA, Rogers PI, DeLong CA. Serial kinematic analysis of the unstable knee after transection of the anterior



- cruciate ligament: temporal and angular changes in a canine model of osteoarthritis. *J Orthop Res* 1994;12(2):229–37.
26. Tashman S, Anderst W, Kolowich P, Havstad S, Arnoczky S. Kinematics of the ACL-deficient canine knee during gait: serial changes over two years. *J Orthop Res* 2004;22(5):931–41.
  27. Tashman S, Anderst WJ. *In vivo* measurement of dynamic joint motion using high speed biplane radiography and CT: application to canine acl deficiency. *J Biomed Eng* 2003;125:238–45.
  28. Treece GM, Prager RW, Gee AH. Regularized marching tetrahedral: improved iso-surface extraction. *Comput Graph* 1999;23:583–98.
  29. Anderst WJ, Tashman S. A method to estimate *in vivo* dynamic articular surface interaction. *J Biomech* 2003;36:1291–9.
  30. Meachim G. Light microscopy of Indian ink preparations of fibrillated cartilage. *Ann Rheum Dis* 1972;31:457–64.
  31. Smith GN, Mickler EA, Albrecht ME, Myers SL, Brandt KD. Severity of medial meniscus damage in the canine knee after anterior cruciate ligament transection. *Osteoarthritis Cartilage* 2002;10:321–6.
  32. Kiviranta I, Tammi M, Jurvelin J, Helminen H. Topographical variation of glycosaminoglycan content and cartilage thickness in canine knee (stifle) joint cartilage. Application of the microspectrophotometric method. *J Anat* 1987;150:265–76.
  33. Brandt KD, Braunstein EM, Visco DM, O'Connor B, Heck D, Albrecht M. Anterior (cranial) cruciate ligament transection in the dog: a bona fide model of osteoarthritis, not merely of cartilage injury and repair. *J Rheumatol* 1991;18(3):436–46.
  34. Vignon E, Arlot M, Hartman D, Moyer B, Ville G. Hypertrophic repair of articular cartilage in experimental osteoarthrosis. *Ann Rheum Dis* 1983;142:82–8.
  35. Brandt KD, Adams ME. Exuberant repair of articular cartilage damage. Effect of anterior cruciate ligament transection in the dog. *Trans Orthop Res Soc* 1989;14:584.
  36. Adams ME, Brandt KD. Hypertrophic repair of canine articular cartilage in osteoarthritis after anterior cruciate ligament transection. *J Rheumatol* 1991;18:428–35.
  37. Braunstein EM, Brandt KD, Albrecht M. MRI demonstration of hypertrophic articular cartilage in osteoarthritis. *Skeletal Radiol* 1990;19:335–9.
  38. Setton LA, Mow VC, Muller FJ, Pita JC, Howell DS. Mechanical properties of canine articular cartilage are significantly altered following transection of the anterior cruciate ligament. *J Orthop Res* 1994;12(4):451–63.
-